

Determination of α_s from a Differential Jet
Multiplicity Distribution at SLC and PEP*

S. Komamiya,¹ F. Le Diberder,¹ G. S. Abrams,² C. E. Adolphsen,³
D. Averill,⁴ J. Ballam,¹ B. C. Barish,⁵ T. Barklow,¹ B. A. Barnett,⁶
J. Bartelt,¹ S. Bethke,² D. Blockus,⁴ G. Bonvicini,⁷ A. Boyarski,¹
B. Brabson,⁴ A. Breakstone,⁸ F. Bulos,¹ P. R. Burchat,³ D. L. Burke,¹
R. J. Cence,⁸ J. Chapman,⁷ M. Chmeissani,⁷ D. Cords,¹ D. P. Coupal,¹
P. Dauncey,⁶ H. C. DeStaebler,¹ D. E. Dorfan,³ J. M. Dorfan,¹
D. C. Drewer,⁶ R. Elia,¹ G. J. Feldman,¹ D. Fernandes,¹ R. C. Field,¹
W. T. Ford,⁹ C. Fordham,¹ R. Frey,⁷ D. Fujino,¹ K. K. Gan,¹ C. Gatto,³
E. Gero,⁷ G. Gidal,² T. Glanzman,¹ G. Goldhaber,² J. J. Gomez Cadenas,³
G. Gratta,³ G. Grindhammer,¹ P. Grosse-Wiesmann,¹ G. Hanson,¹
R. Harr,² B. Harral,⁶ F. A. Harris,⁸ C. M. Hawkes,⁵ K. Hayes,¹ C. Hearty,²
C. A. Heusch,³ M. D. Hildreth,¹ T. Himel,¹ D. A. Hinshaw,⁹ S. J. Hong,⁷
D. Hutchinson,¹ J. Huyen,⁶ W. R. Innes,¹ R. G. Jacobsen,¹ J. A. Jaros,¹
C. K. Jung,¹ J. A. Kadyk,² J. Kent,³ M. King,³ S. R. Klein,¹ D. S. Koetke,¹
W. Koska,⁷ L. A. Kowalski,¹ W. Kozanecki,¹ J. F. Kral,² M. Kuhlen,⁵
L. Labarga,³ A. J. Lankford,¹ R. R. Larsen,¹ M. E. Levi,² A. M. Litke,³
X. C. Lou,⁴ V. Lüth,¹ J. A. McKenna,⁵ J. A. J. Matthews,⁶ T. Mattison,¹
B. D. Milliken,⁵ K. C. Moffeit,¹ C. T. Munger,¹ W. N. Murray,⁴
J. Nash,¹ H. Ogren,⁴ K. F. O'Shaughnessy,¹ S. I. Parker,⁸ C. Peck,⁵
M. L. Perl,¹ F. Perrier,¹ M. Petradza,⁷ R. Pitthan,¹ F. C. Porter,⁵
P. Rankin,⁹ K. Riles,¹ F. R. Rouse,¹ D. R. Rust,⁴ H. F. W. Sadrozinski,³
M. W. Schaad,² B. A. Schumm,² A. Seiden,³ J. G. Smith,⁹ A. Snyder,⁴
E. Soderstrom,⁵ D. P. Stoker,⁶ R. Stroynowski,⁵ M. Swartz,¹ R. Thun,⁷
R. Van Kooten,¹ P. Voruganti,¹ S. R. Wagner,⁹ S. Watson,³ P. Weber,⁹
A. Weigend,¹ A. J. Weinstein,³ A. J. Weir,⁵ E. Wicklund,⁵ M. Woods,¹
D. Y. Wu,⁵ M. Yurko,⁴ C. Zaccardelli,³ and C. von Zanthier³

PACS numbers: 12.38.Qk, 13.87-a

Submitted to *Physical Review Letters*.

* This work was supported in part by Department of Energy contracts DE-AC03-81ER40050 (CIT), DE-AM03-76SF00010 (UCSC), DE-AC02-86ER40253 (Colorado), DE-AC03-83ER40103 (Hawaii), DE-AC02-84ER40125 (Indiana), DE-AC03-76SF00098 (LBL), DE-AC02-84ER40125 (Michigan), and DE-AC03-76SF00515 (SLAC), and by the National Science Foundation (Johns Hopkins).

¹*Stanford Linear Accelerator Center, Stanford University,
Stanford, California 94309*

²*Lawrence Berkeley Laboratory and Department of Physics,
University of California, Berkeley, California 94720*

³*University of California, Santa Cruz, California 95064*

⁴*Indiana University, Bloomington, Indiana 47405*

⁵*California Institute of Technology, Pasadena, California 91125*

⁶*Johns Hopkins University, Baltimore, Maryland 21218*

⁷*University of Michigan, Ann Arbor, Michigan 48109*

⁸*University of Hawaii, Honolulu, Hawaii 96822*

⁹*University of Colorado, Boulder, Colorado 80309*

ABSTRACT

We measure the differential jet multiplicity distribution in e^+e^- annihilation with the Mark II detector. This distribution is compared with the second order QCD prediction and α_s is determined to be $0.123 \pm 0.009 \pm 0.005$ at $\sqrt{s} \approx M_Z$ (at SLC) and $0.149 \pm 0.002 \pm 0.007$ at $\sqrt{s} = 29$ GeV (at PEP). The running of α_s between these two center of mass energies is consistent with the QCD prediction.

The study of jets provides an important laboratory to probe the hard (large momentum transfer) interactions of quarks and gluons. With increasing the center-of-mass energy of these hard processes, perturbative QCD effects which were masked by fragmentation effects at lower energies become more visible. One of the main experimental issues for jet analyses is the measurement of the QCD scale parameter $\Lambda_{\overline{MS}}$, which determines the coupling strength of the strong interaction at any given mass scale (Q^2). In determining $\Lambda_{\overline{MS}}$ (or α_s), it is better to use observables which are insensitive to fragmentation and higher order QCD effects. In that respect, the commonly used observables are (1) the total hadronic cross section (σ_{tot}), (2) the energy-energy-correlation asymmetry and (3) the three-jet-event fraction. However, σ_{tot} is not easy to measure precisely enough to determine $\Lambda_{\overline{MS}}$ because the QCD effect is small (approximately 5% of σ_{tot}). The energy-energy-correlation asymmetry is not free from systematic effects associated with fragmentation and hence extensive studies of these effects are needed to estimate the corresponding systematic errors.¹ The three-jet event fraction appears relatively insensitive to fragmentation effects, if one chooses a reasonable jet algorithm and if one deals only with hard three-jet events.² However, the actual dependence of the three-jet event fraction on the jet resolution parameter (y_{cut}) used to select hard three-jet events is not statistically easy to handle. This problem can be solved by using a differential jet multiplicity as described below.

The purpose of this paper is to present determinations of α_s at two different center-of-mass energies, at SLC and at PEP. The analysis is performed using the same Mark II detector configuration at both energies and applying the same technique, based on the differential jet multiplicity.

The Mark II detector has been described in detail elsewhere.³⁻⁵ In this ana-

lysis, the main drift chamber, barrel and endcap electromagnetic calorimeters are used. We analyse the data which were collected after the installation of the new drift chamber and of the endcap shower detector at PEP.³ The triggers for hadronic events at SLC and at PEP are given elsewhere.^{3,4} Trigger efficiencies are close to 100% for multihadronic events so that the analysis is not significantly affected by trigger biases. Events are selected by requiring that the number of charged tracks is at least seven at SLC [at least five at PEP] and that the sum of charged and neutral particle energies (E_{vis}) is greater than $0.50 \sqrt{s}$ at SLC [$0.55 \sqrt{s}$ at PEP]. In order to reduce the bias due to initial state radiation and background from two photon processes for the PEP data, events with large missing energy or with a large energy photon are eliminated by applying additional cuts described in Ref.3. For the Z -resonance data such effects are small, hence we do not apply any cuts other than those mentioned above.⁴ The detection efficiency for multihadron events is estimated using QCD-based Monte Carlo generators⁶⁻⁸ to be 0.80 ± 0.02 at SLC [0.51 ± 0.02 at PEP]. The integrated luminosities used in the analysis are 19 nb^{-1} at SLC and 27 pb^{-1} at PEP. A total of 391 events from the SLC data and 7348 events from the PEP data pass the selection cuts.

The parton shower models^{6,7} are very attractive because they describe the data very well over a wide range of center-of-mass energy using the same parameters,⁹ but $\Lambda_{\overline{MS}}$ cannot be uniquely defined in these models which are based on a leading-log approximation. Therefore these models are used only for studying detector effects and for determining efficiencies. Second order perturbative QCD predictions are directly compared with the data for testing the hard QCD processes and for determining α_s .

We use the algorithm proposed by the JADE collaboration to define the number

of jets (jet multiplicity) in an event.¹⁰ The algorithm proceeds as follows:

for each particle (cluster) pair i, j , the scaled invariant mass

$$y_{ij} = \frac{2E_i E_j (1 - \cos \chi_{ij})}{E_{\text{vis}}^2}$$

is calculated, where E_i and E_j are the energy of the particles (clusters) and χ_{ij} is the angle between them. The particle (or cluster) pair with the smallest y_{ij} is combined by adding the 4-momenta of the two particles (clusters) i and j to form a new cluster $i + j$ ($p_{i+j}^\mu = p_i^\mu + p_j^\mu$). The above clustering procedure is repeated until all the clusters satisfy the condition $y_{ij} > y_{\text{cut}}$ where y_{cut} is referred to as the jet resolution. The three-jet fraction $f_3(y_{\text{cut}})$ is defined to be the number of three-jet events obtained with the algorithm, divided by the total number of hadronic events. The two-jet fraction $f_2(y_{\text{cut}})$ and the four jet fraction $f_4(y_{\text{cut}})$ are similarly defined.¹¹ This jet algorithm has the important feature that mapping from parton jets to hadron jets in Monte Carlo hadronic events is close to one-to-one for reasonably large y_{cut} (≥ 0.04) values.² However, it is not easy to extract α_s by fitting the $f_3(y_{\text{cut}})$ (or $f_2(y_{\text{cut}})$) distribution because the same events contribute at different y_{cut} values and one must take into account all the correlations in this distribution.

To overcome this difficulty, a differential jet multiplicity is defined in the following way. The clustering is terminated when the number of jets has reached a pre-selected value n , irrespective of y_{ij} values. For each event, particles are assigned to n -jets using this method and y_n is defined to be the minimum value of the y_{ij} 's ($i \neq j$, $i, j = 1, 2, \dots, n$). In other words, y_n is the y_{cut} value corresponding to the transition from n -jet to $(n - 1)$ -jet for a given event. The distribution function of y_n is denoted $g_n(y_n)$. Integrating $g_3(y_3)$ over y_3 from 0 to y_{cut} , one recovers

$f_2(y_{cut})$ because all the events with $y_3 < y_{cut}$ are categorized as two-jet events for the given jet resolution y_{cut} . Hence,

$$g_3(y_3)|_{y_3=y_{cut}} = \frac{\partial}{\partial y_{cut}} f_2(y_{cut}).$$

Similarly,

$$g_4(y_4)|_{y_4=y_{cut}} = \frac{\partial}{\partial y_{cut}} [f_2(y_{cut}) + f_3(y_{cut})].$$

Note that only the leading term ($\propto \alpha_s^2$) is available for g_4 in second order QCD calculations. Therefore we restrict our analysis to the differential jet fraction $g_3(y_3)$ to determine α_s .

Detector effects, biases due to event selection and initial state radiation effects are corrected with bin-by-bin correction factors. In the range $0.04 \leq y_3 \leq 0.14$, the corrections are typically less than 5% for SLC data [10% for PEP data]. The bin-to-bin systematic errors due to the variation of the correction factors for various models⁶⁻⁸ are less than 4% at SLC [3% at PEP]. These errors slightly increase with y_3 . The overall normalization uncertainty in the correction factors is estimated to be 2% at SLC [3% at PEP]. The corrected $g_3^{corr}(y_3)$ distributions for the two data samples are shown in Fig.1. Also shown in the figure are the QCD predictions for three $\Lambda_{\overline{MS}}$ values, as obtained by differentiating the function f_2 calculated by Kramer and Lampe, in the \overline{MS} scheme, for $y_3 < 0.14$.¹² The shape of the distributions, which depends only slightly on $\Lambda_{\overline{MS}}$, is well described by the QCD predictions.

Corrections are not applied for fragmentation effects. Rather, they are accounted for as systematic errors. These errors are estimated as follows. Using the same jet algorithm, and for a given fragmentation model, the distributions

of y_3 at the parton level ($g_3^{partons}$) and after fragmentation ($g_3^{hadrons}$) are obtained. The systematic errors are then derived, for a given y_3 , from the differences $|g_3^{partons} - g_3^{hadrons}|$ for various models.⁶⁻⁸ In Fig.2, the ratio $g_3^{partons}/g_3^{hadrons}$ is shown as a function of y_3 for two models.^{6,8} In the range $0.04 \leq y_3 \leq 0.14$, the bin-to-bin systematic errors associated with fragmentation effects are 3-5% at SLC [5-10% at PEP]. The normalization uncertainty is estimated to be 2% at SLC [4% at PEP].¹⁴ The systematic errors estimated by varying the fragmentation parameters are significantly smaller than the errors mentioned above.

The α_s value is obtained from a fit of the corrected $g_3(y_3)$ distribution to the $\mathcal{O}(\alpha_s^2)$ QCD prediction.¹² The fit is performed within the range of $0.04 \leq y_3 \leq 0.14$ using a likelihood method which accounts for the statistical errors and the various systematic errors. The lower y_3 limit of the fitted range is chosen in order to limit the fragmentation effects, while the upper limit arises only because the QCD prediction for $y_3 > 0.14$ is not available in Ref.12. Choosing the renormalization point Q^2 to be s , we obtain

$$\alpha_s = 0.123 \pm 0.009 \pm 0.005 \quad \text{at SLC,}$$

$$\alpha_s = 0.149 \pm 0.002 \pm 0.007 \quad \text{at PEP.}$$

The running of α_s from 29 GeV to 91 GeV is consistent with the QCD prediction, as shown in Fig.3. The running of α_s with Q^2 is governed by the Renormalization Group Equation (RGE) which, to second order in α_s , is given by

$$\frac{\partial}{\partial \ln Q^2} \frac{\alpha_s}{2\pi} = -b_0 \left(\frac{\alpha_s}{2\pi}\right)^2 \left(1 + b_1 \frac{\alpha_s}{2\pi}\right) .$$

The coefficients b_0 and b_1 do not depend on the renormalization scheme chosen, hence they represent fundamental physical quantities. Denoting by n_f the effective

number of flavors at a given Q^2 , QCD predicts $b_0 = (33 - 2n_f)/6$ and $b_1 = (153 - 19n_f)/(33 - 2n_f)$. The RGE can be integrated to express b_0 in terms of our two measurements of the coupling constant α_s^{SLC} and α_s^{PEP} and of the $\ln Q^2$ variation $\Delta \ln Q^2 = 2 \ln(91/29) = 2.29$. One gets

$$b_0 = \frac{F(\alpha_s^{SLC}) - F(\alpha_s^{PEP})}{\Delta \ln Q^2} ,$$

$$\text{with } F(\alpha_s) = \frac{2\pi}{\alpha_s} - b_1 \ln\left(\frac{2\pi}{\alpha_s} + b_1\right) .$$

This formula leads to $b_0 = 3.4_{-1.4}^{+2.1}$ where the errors take into account the partial cancellation of the normalization uncertainties. This value, which is almost independent of b_1 , is in good agreement with the QCD prediction of $b_0 = 3.83$ for $n_f = 5$.

To express the α_s measurements in terms of the QCD scale parameter $\Lambda_{\overline{MS}}$, we use the approximate solution of the RGE given in Ref.13. We obtain $\Lambda_{\overline{MS}} = 0.29_{-0.12-0.06}^{+0.17+0.11}$ GeV at SLC, and $\Lambda_{\overline{MS}} = 0.28_{-0.02-0.07}^{+0.02+0.08}$ GeV at PEP, in agreement with the value $0.33 \pm 0.04 \pm 0.07$ GeV previously obtained using the energy-energy-correlation by Mark II at 29 GeV.¹

In finite order perturbative calculations, there is an ambiguity due to the renormalization scale Q^2 . Recently, triggered by the work of Kramer and Lampe,¹⁵ several experimental papers were published in an attempt to optimize Q^2 for the determination of $\Lambda_{\overline{MS}}$.¹⁶⁻¹⁸ The simultaneous determination of Q^2 and $\Lambda_{\overline{MS}}$ using jet multiplicity favors very small Q^2 values,¹⁸ but the result is very sensitive to the four-jet fraction which does not have the next-to-leading order term in the $\mathcal{O}(\alpha_s^2)$ calculation. If a variable with next-to-leading order terms is used, the Q^2 ambiguity is large. Several prescriptions have been proposed to assign Q^2 a particular value.¹⁹⁻²¹ For the purpose of illustrating and exploring the effect of the

choice of Q^2 , we use the Brodsky-Lepage-Mackenzie (BLM) method²¹ to eliminate the Q^2 ambiguity for g_3 at each y_3 value. The Q value prescribed by the BLM method (Q^*) is 4 GeV [1.3 GeV] at $y_3 = 0.05$ and increases to 6 GeV [2.0 GeV] at $y_3 = 0.10$ for $\sqrt{s} = 91$ GeV [$\sqrt{s} = 29$ GeV]. In this picture, the smallness of Q^2 might be understood in terms of the typical momentum scale involved in the vacuum polarization loops; the energy scale is related to the allowable invariant mass (virtuality) of gluons, which can be as small as a few GeV. Choosing $Q^2 = (Q^*)^2$ at each value of y_3 and \sqrt{s} , and n_f values appropriate to the small Q^* values ($n_f = 4$ for SLC and $n_f = 3$ for PEP), the $\Lambda_{\overline{MS}}$ values obtained using the BLM method are $0.17_{-0.06}^{+0.08+0.05}$ GeV at SLC and $0.17_{-0.01}^{+0.01+0.03}$ GeV at PEP. The range of the $\Lambda_{\overline{MS}}$ values discussed in the letter implies that the uncertainty on this measurement induced by the Q^2 ambiguity is far in excess of the systematic errors arising from the fragmentation effects.

In conclusion, we have presented the measurement of the coupling strength of the strong interaction in e^+e^- annihilation at $\sqrt{s} \approx M_Z$ (SLC) and at $\sqrt{s} = 29$ GeV (PEP) using the differential jet multiplicity g_3 . The method is relatively insensitive to fragmentation effects and statistically easy to handle. In the framework of second order QCD calculations and for $Q^2 = s$, the measured values of α_s are $0.123 \pm 0.009 \pm 0.005$ at $\sqrt{s} = 91$ GeV and $0.149 \pm 0.002 \pm 0.007$ at $\sqrt{s} = 29$ GeV. The running of α_s from 29 GeV to 91 GeV is seen and is consistent with the QCD prediction. The corresponding values of the QCD scale parameter are $\Lambda_{\overline{MS}} = 0.29_{-0.12}^{+0.17+0.11}$ GeV at SLC, and $\Lambda_{\overline{MS}} = 0.28_{-0.02}^{+0.02+0.08}$ GeV at PEP. For comparison, results have been also presented at considerably smaller values of the renormalization point (Q^2), as suggested, for example, by the Brodsky-Lepage-Mackenzie method.

REFERENCES

1. Mark II Collab., D.R. Wood et al., Phys. Rev. D**37**, 3091 (1988).
2. JADE Collab., S. Bethke et al., Phys. Lett. B**213**, 235 (1988); Mark II Collab., S. Bethke et al., Z. Physik C**43**, 325 (1989).
3. Mark II Collab., A. Petersen et al., Phys. Rev. D**37**, 1 (1988).
4. Mark II Collab., G.S. Abrams et al., Phys. Rev. Lett. **63**, 1558 (1989); SLAC-PUB-5092, to be submitted to Phys. Rev. Lett.
5. Mark II Collab., G.S. Abrams et al., Nucl. Instrum. Methods. A**281**, 55 (1989).
6. T. Sjöstrand, Comp. Phys. Comm. **39**, 347 (1986); T. Sjöstrand and M. Bengtsson, Comp. Phys. Comm. **43**, 367 (1987).
7. G. Marchesini and B.R. Webber, Nucl. Phys. B**238**, 1 (1984); B. R. Webber, Nucl. Phys. B**238**, 492 (1984).
8. T.D. Gottschalk and M. P. Shatz, Phys. Lett. B**150**, 451 (1985); CALT-68-1172,-1173 (1985).
9. Ref.3 , Ref.4 and references therein.
10. JADE Collab., W. Bartel et al., Z. Physik, C**33**, 23 (1986).
11. We use the notation f_n for the n -jet-event fraction instead of R_n because the latter notation can be confused with $\frac{\sigma_{n-jet}}{\sigma_{\mu^+\mu^-}}$.
12. G. Kramer and B. Lampe, Fortschr. Phys. **37**, 161 (1989).
13. Particle Data Group, M. Aguilar-Benitez et al., Phys. Lett. B**170**, 78 (1986).
14. For independent fragmentation models the fragmentation effects are larger (10% at SLC and 20% at PEP).

15. G. Kramer and B. Lampe, Z. Physik, **C39**, 101 (1988).
16. N. Magnussen, PhD thesis, Universität Wuppertal, 1988.
17. CELLO Collab., H.J. Behrend et al., Z.Phys. **C44**, 63 (1989).
18. S. Bethke, Z. Physik, **C43**, 331 (1989); AMY Collab., I.H. Park et al., KEK-89-53, submitted to the Lepton Photon Symposium (Stanford, 1989).
19. G. Grunberg, Phys. Lett. **B95**, 70 (1980).
20. P.M. Stevenson, Phys. Rev. **D23**, 2916 (1981).
21. S. Brodsky, G.P. Lepage and P.B. Mackenzie, Phys. Rev. **D28**, 228 (1983).

FIGURE CAPTIONS

- Fig. 1 The experimental distributions of y_3 at (a) $\sqrt{s} = 91$ GeV, and (b) $\sqrt{s} = 29$ GeV. Only the statistical errors are indicated in the figures. The curves below $y_3 = 0.14$ indicate the QCD predictions with $\Lambda_{\overline{MS}} = 0.1$ GeV, 0.3 GeV and 0.5 GeV for $Q^2 = s$. The y_3 range used in the fit for the determination of α_s is defined by the two dashed lines. The curves above $y_3 = 0.14$ are extrapolated from the QCD predictions in the low y_3 range.
- Fig. 2 The ratio $g_3^{partons}/g_3^{hadrons}$ as a function of y_3 for partons and for hadrons (after fragmentation and decay of unstable particles) at (a) $\sqrt{s} = 91$ GeV, and (b) $\sqrt{s} = 29$ GeV. The solid curve corresponds to the Lund model based on $\mathcal{O}(\alpha_s^2)$ matrix element and the dashed curve to the Lund parton shower model. The error bars indicate the Monte Carlo statistical errors.
- Fig. 3 The strong coupling $\alpha_s(Q^2 = s)$ as a function of \sqrt{s} . The errors include statistical and systematic uncertainties added in quadrature. Also shown are the extrapolations of the α_s measurement at $\sqrt{s} = 29$ GeV to higher energies using the formula of Ref.13, or assuming a constant α_s . The dotted lines indicate the extrapolation of the measured $\alpha_s \pm 1\sigma$ from 29 GeV.

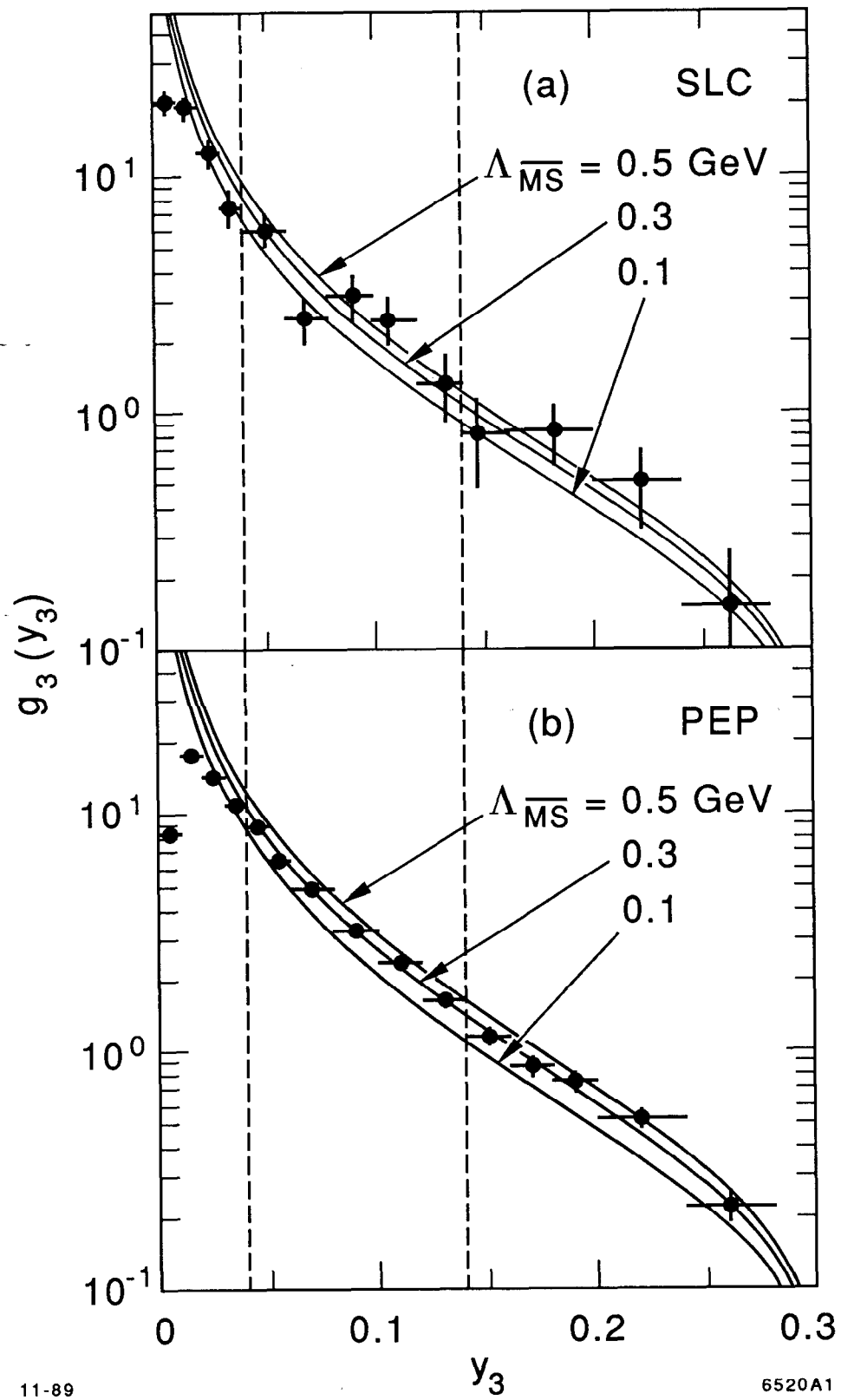


Fig. 1

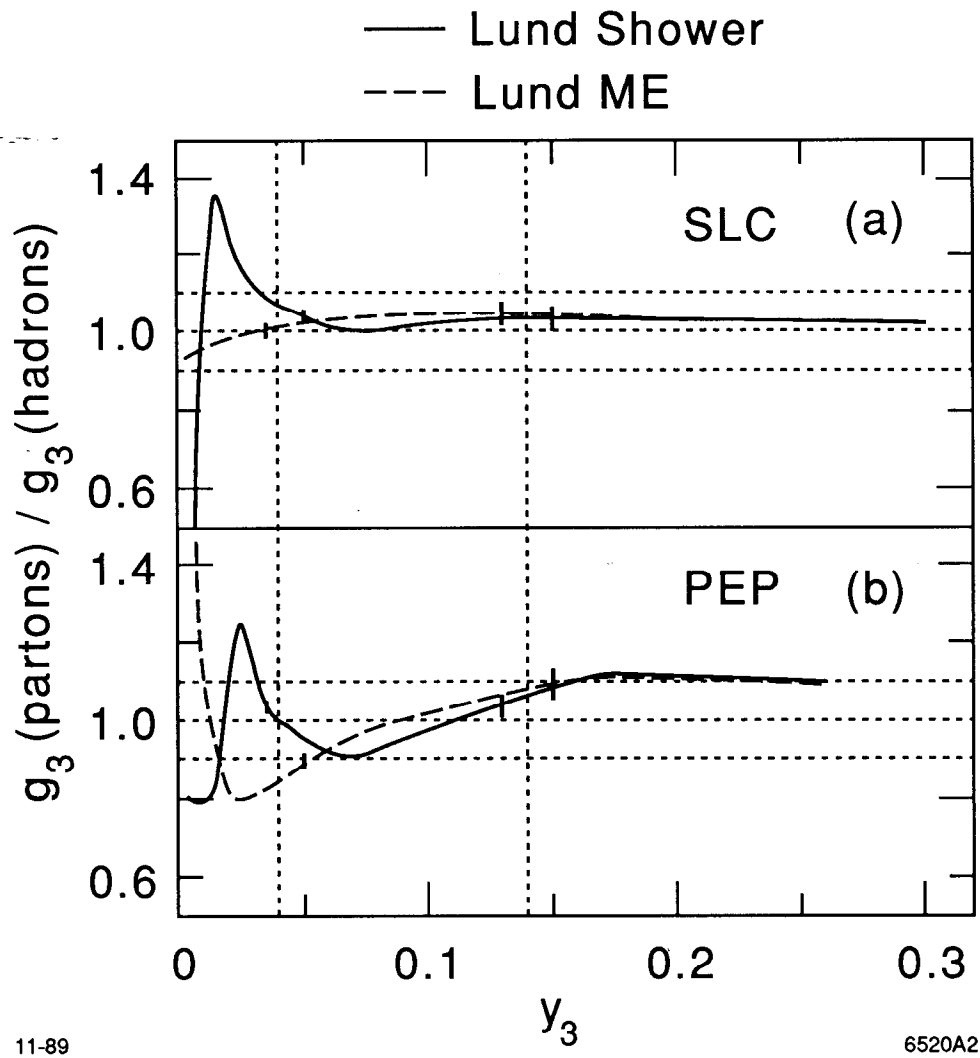
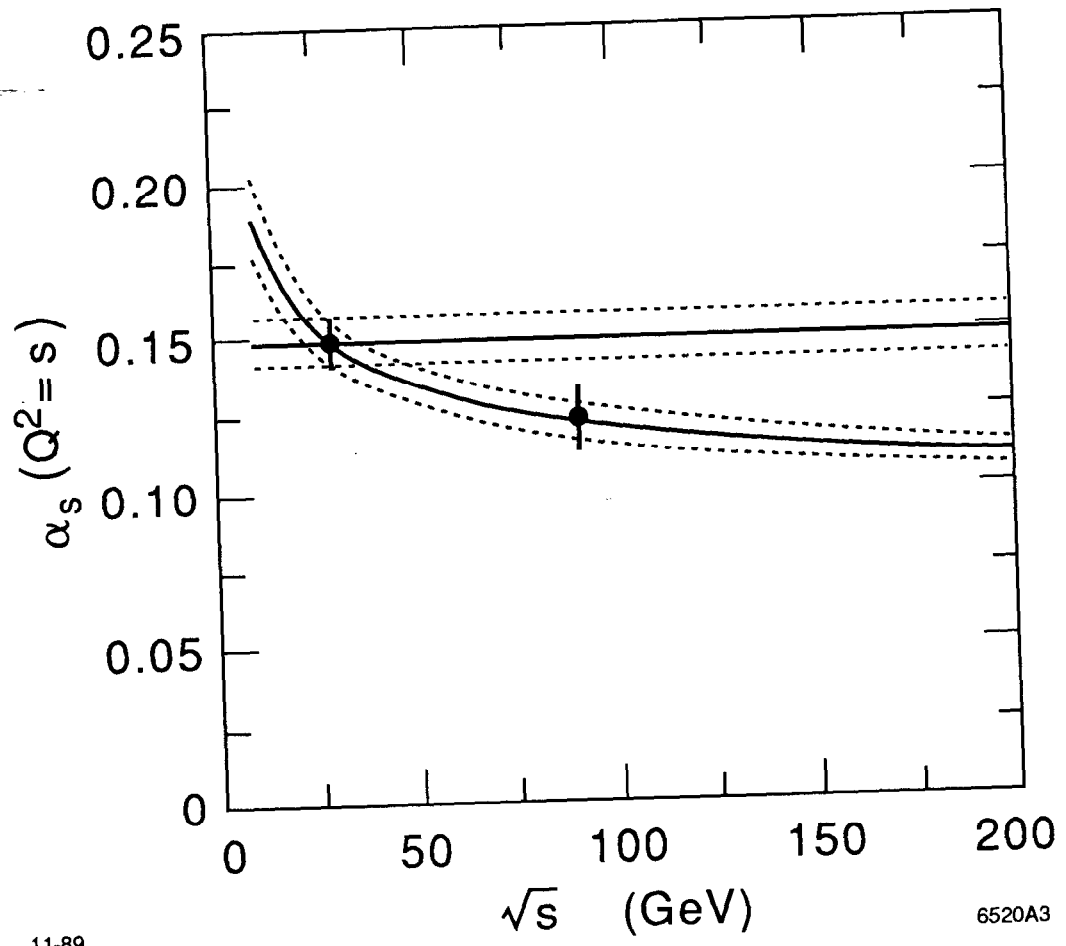


Fig. 2



11-89

6520A3

Fig. 3